Electronic Supplementary Information

Bioconjugated fluorescent organic nanoparticles targeting EGFR-overexpressing cancer cells

Adrien Faucon,[a] Houda Benhelli-Mokrani,[b] Fabrice Fleury,[b] Stéphanie Dutertre,[c] Marc Tramier,[c,d] Joanna Boucard,[a] Lénaïc Lartigue,[a] Steven Nedellec,[e] Philippe Hulin,[e] and Eléna Ishow[a]*

[a]CEISAM–UMR CNRS 6230, Université de Nantes, 2 rue de la Houssinière, 44322 Nantes, France. [b]UFIP–UMR CNRS 6286, Université de Nantes, 2 rue de la Houssinière, 44322 Nantes, France. [c]Microscopy Rennes Imaging Center (MRIC), Biosit – UMS CNRS 3480/US INSERM 018, University of Rennes 1, 35043 Rennes, France. [d]Institut de Génétique et Développement de Rennes, UMR CNRS 6290, Université de Rennes 1, 2 avenue du Pr Léon Bernard, 35043 Rennes, France. [e]INSERM UMS 016-UMS CNRS 3556, 8 quai Moncousu, 44007 Nantes, France. E-mail: elena.ishow@univ-nantes.fr

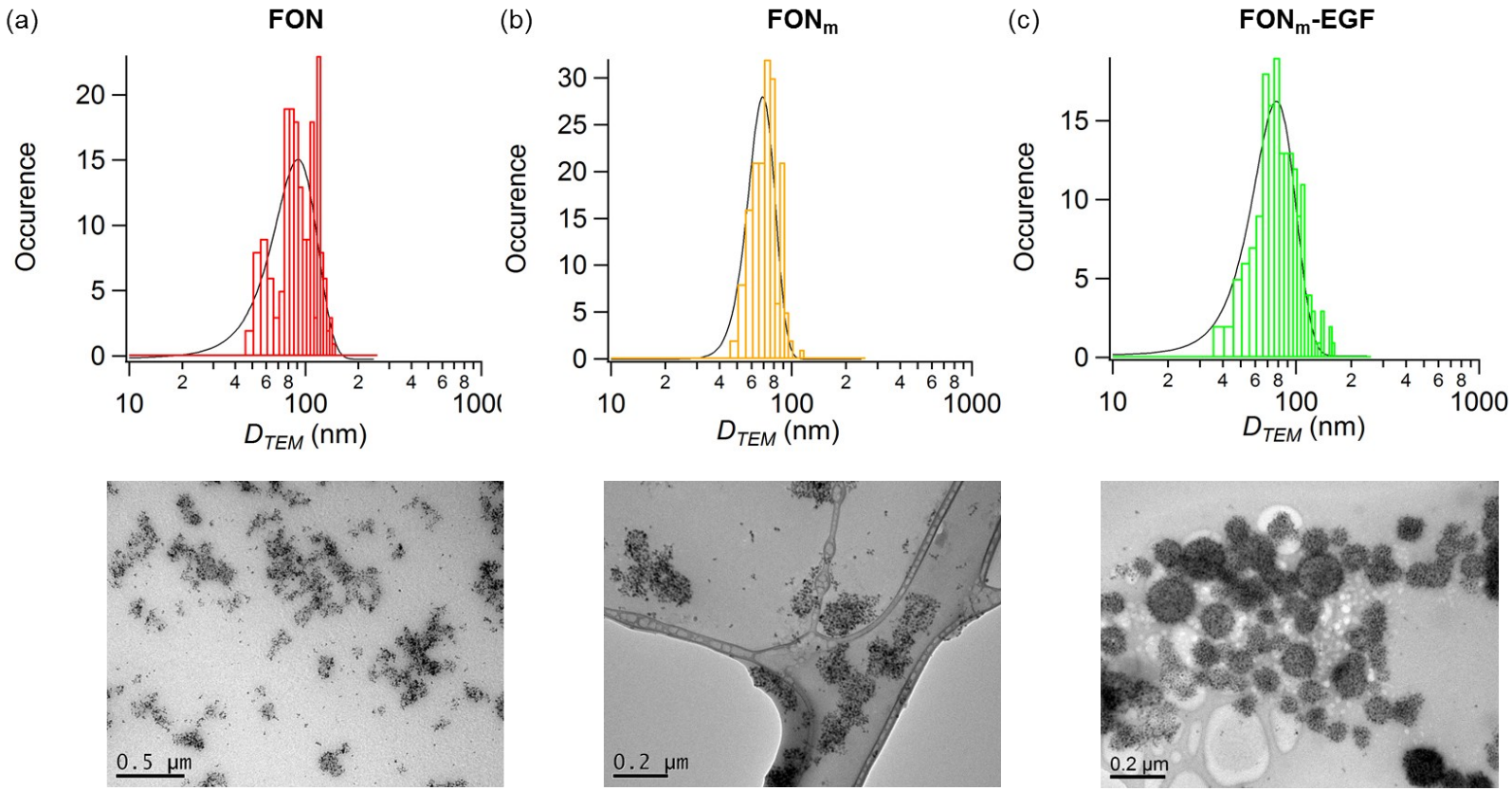

Fig. S1 TEM diameter distributions for (a) FON, (b) FON_m and (c) FON_m-EGF nanoassemblies from TEM imaging after sample deposition on holey carbon grid. Histograms were traced using a 5 nm segmentation and fitted with Gaussian distribution (continuous black line)

.

Magnetic measurements

Magnetic measurements were collected with a Quantum Design MPMS-XL5 SQUID magnetometer. The nanoassembly solutions were diluted and deposited on a small piece of cotton to avoid magnetic dipole−dipole interactions (iron concentration in the 4 - 8×10^{-5} mol.L^{-1} range). After water evaporation, the sample was placed in a polycarbonate capsule and the magnetization curves were measured at 300 K with a magnetic field varying from 0 to 3 T. All data were carefully corrected from diamagnetic contributions due to the sample holder and container

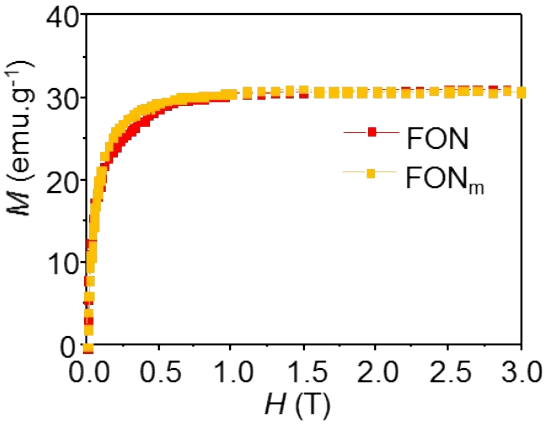

Fig. S2 First magnetization curves at 300 K of FON and FON_m nanossemblies as a function of the applied magnetic field.

Table S1 Structural and photophysical characteristics of FON_m, FON_m-cys, and FON_m-trityl.

sample	λ^{max}(abs) (nm)	λ^{max}(em) (nm)	Φ_f ($\times 10^{-2}$)	$<\tau_S>^b$ (ns)
FON_m	426	611	1.4	1.22
FON_m-cys	426	608	2.2	1.51
FON_m-trityl	426	597	2.8	2.02

[a] Measured in HBSS solution. [b] Average amplitude excited state lifetime calculated from the multi-exponential decay using a global fit analysis after $I_f(t) = \sum_i a_i \exp(-t/\tau_i)$ with $\langle \tau_S \rangle = \frac{\sum_i a_i \tau_i}{\sum_i a_i}$ amplitude-weighted excited state average lifetime.

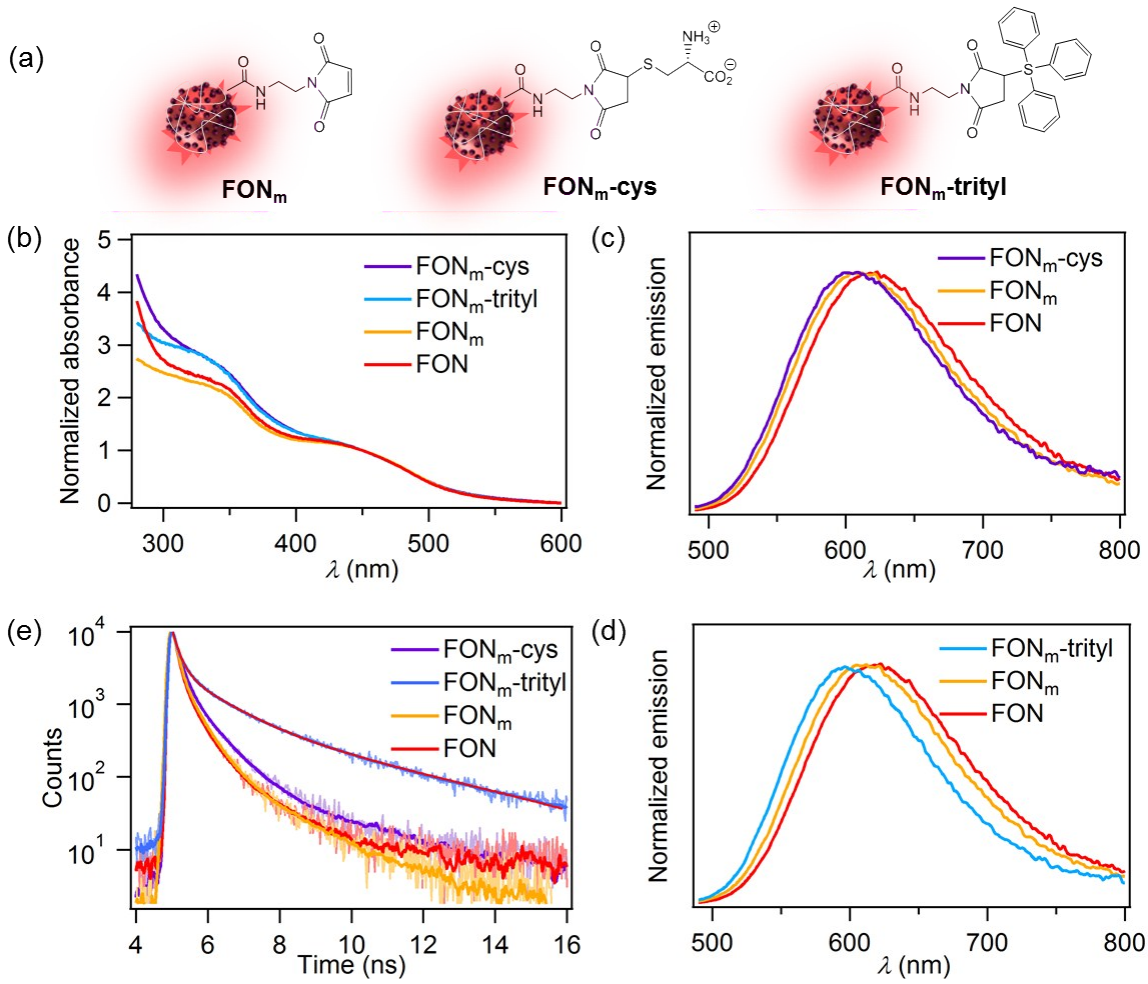

Fig. S3 (a) Schematic structures of the nanoassemblies after reacting cystein (FON_m-cys) and triphenylmethanethiol (FON_m-trityl) with FON_m. (b) Absorption spectra, (c) and (d) emission spectra (λ_{exc} = 450 nm), and fluorescence decay (λ_{exc} = 450 nm, λ_{exc} = 610 nm) of FON_m-cys, FON_m-trityl, FON_m and FON.

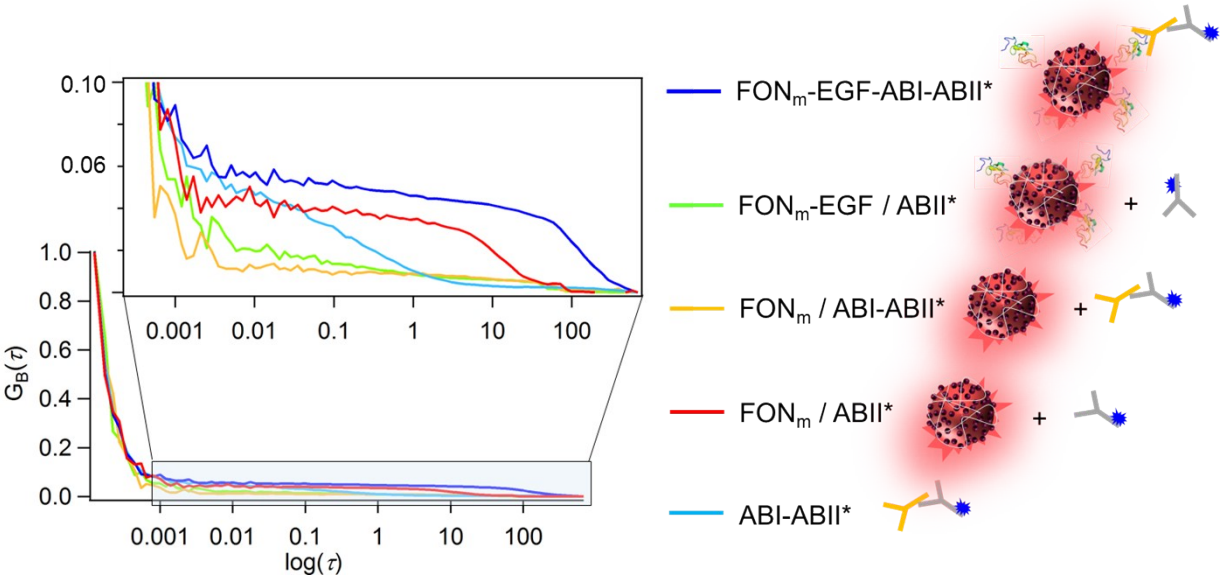

Fig. S4 Autocorrelograms of the fluorescence intensity fluctuations recorded in the blue channel (415-455 nm) over 6 min upon excitation at 405 nm for the immunoconstruct FON$_m$-EGF-ABI-ABII*, FON$_m$-EGF/ABII*, FON$_m$/ABI-ABII*, FON$_m$/ABII*, an ABI-ABII*. Inset: zoom-in.

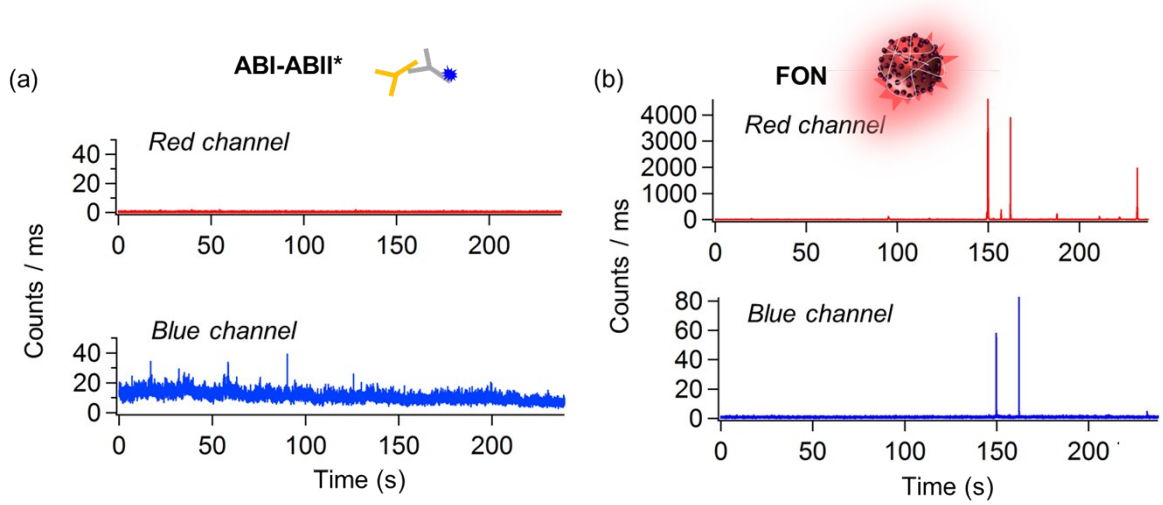

Fig. S5 Fluorescence intensity time traces of control solutions recorded in the red (581-654 nm) and blue (415-455 nm) channels over 6 min upon excitation at 405 nm: (a) ABI-ABII*, (b) FON.

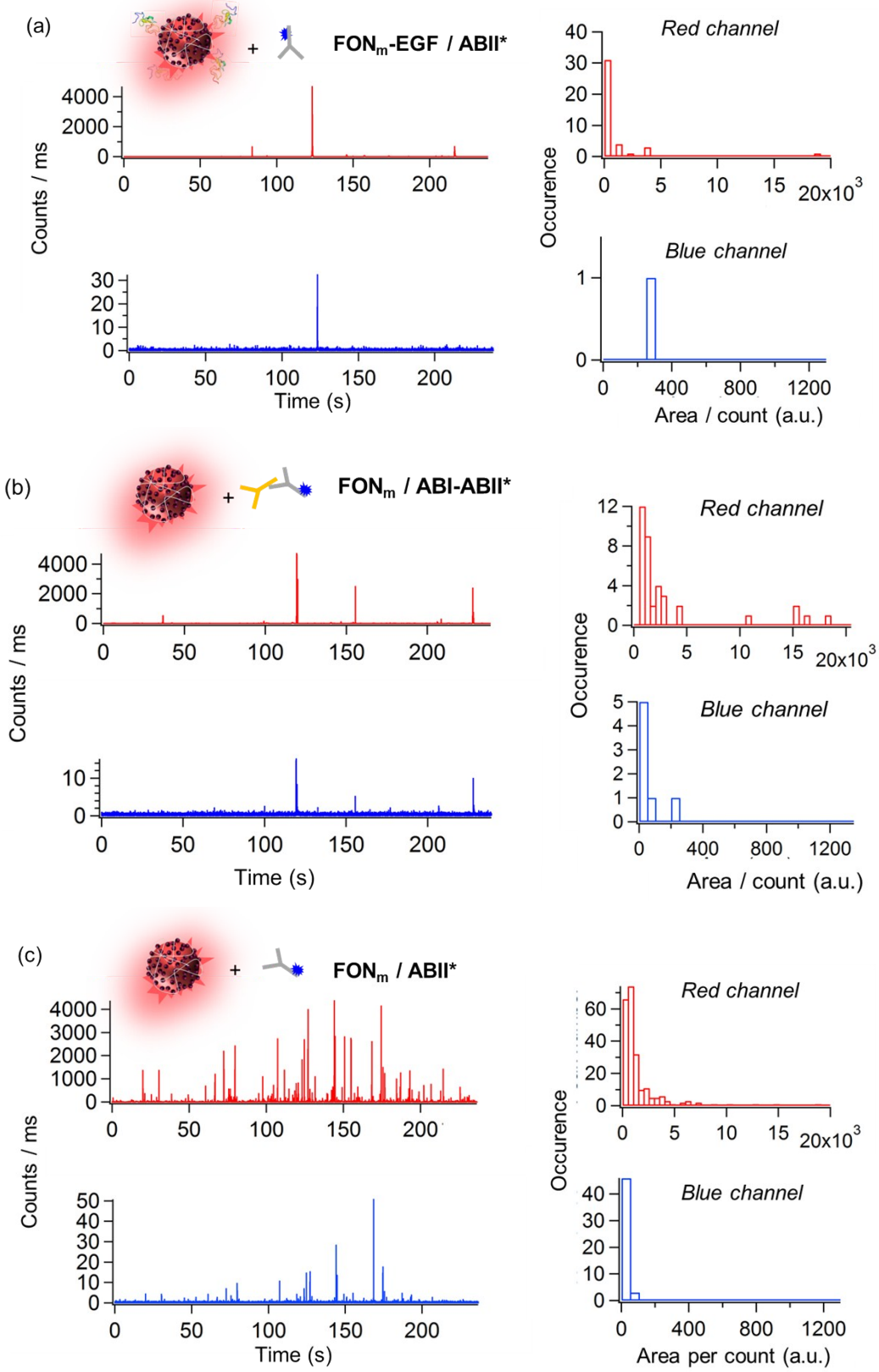

Fig. S6 Fluorescence intensity time traces and corresponding histograms of the peak areas recorded in the red (581-654 nm) and blue (415-455 nm) channels over 6 min. upon excitation at 405 nm for the control experiments: (a) FON$_m$-EGF/ABI-ABII*, (b) FON$_m$/ABI-ABII* and (c) FON$_m$/ABII*.

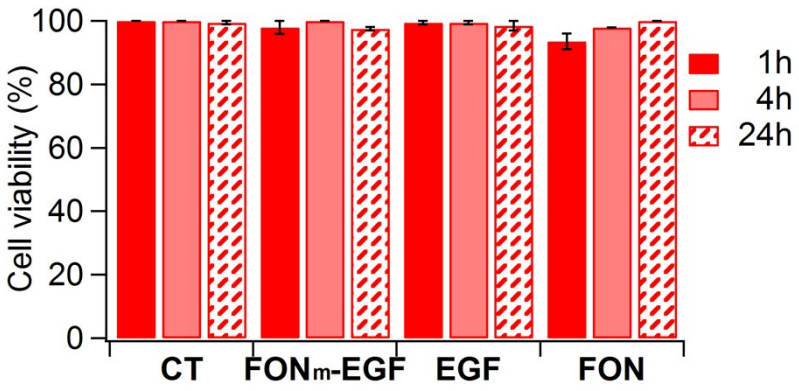

Fig. S7 Cell viability using trypan blue exclusion test for MDA-MB-468 cancer cells incubated with FON_m-EGF, EGF (10 ng.mL^{-1}), and FON in culture medium supplemented with FBS after 1 h, 4 h, and 24 h incubation times.